

NSTX-U RESEARCH ADVANCING THE PHYSICS OF SPHERICAL TOKAMAKS

J.W. BERKERY¹, P.O. ADEBAYO-IGE², H. AL KHAWALDEH³, G. AVDEEVA⁴, S.-G. BAEK⁵, S. BANERJEE¹, K. BARADA⁶, D.J. BATTAGLIA⁷, R.E. BELL¹, E. BELLI⁴, E.V. BELOVA¹, N. BERTELLI¹, N. BISAI⁸, P.T. BONOLI⁵, M.D. BOYER⁷, J. BUTT⁹, J. CANDY⁴, C.S. CHANG¹, C.F. CLAUSER⁵, L.D. CORONA RIVERA¹, M. CURIE⁹, P.C. DE VRIES¹⁰, R. DIAB⁵, A. DIALLO¹, J. DOMINSKI¹, V. DUARTE¹, E. EMDEE¹, N.M. FERRARO¹, R. FITZPATRICK¹¹, E.L. FOLEY¹², E. FREDRICKSON¹, M. GALANTE¹², K.F. GAN², S. GERHARDT¹, R. GOLDSTON¹, W. GUTTENFELDER^{1,13}, R. HAGER¹, M.O. HANSON⁷, S.C. JARDIN¹, S.M. KAYE¹, A. KHODAK¹, J. KINSEY¹⁴, A. KLEINER¹, E. KOLEMEN⁹, S. KU¹, M. LAMPERT¹, B. LEARD³, B.P. LEBLANC¹, F.M. LEVINTON¹², C. LIU¹, T. LOOBY⁷, T. MACWAN⁶, R. MAINGI¹, J. MCCLENAGHAN⁴, J. MENARD¹, S. MUNARETTO¹, M. ONO¹, A. PAJARES⁴, J. PARISI¹, J.-K. PARK^{1,15}, M.S. PARSONS¹, B.S. PATEL¹⁶, M. PODESTÀ¹, F. POLI¹, M. PORCELLI⁹, T. RAFIQ³, S. SABBAGH¹⁷, Á. SÁNCHEZ VILLAR¹, E. SCHUSTER³, J. SCHWARTZ^{1,8}, A. SHARMA¹, S. SHIRAIWA¹, P. SINHA¹, D. SMITH¹⁸, S. SMITH⁴, V.A. SOUKHANOVSKII¹⁹, G. STAEBLER²⁰, E. STARTSEV¹, B. STRATTON¹, K.E. THOME⁴, W. TIERENS²⁰, M. TOBIN¹⁷, I.U. UZUN-KAYMAK¹², B. VAN COMPERNOLLE⁴, J. WAI⁷, W. WANG¹, W. WEHNER⁴, A. WELANDER⁴, J. YANG¹, V. ZAMKOVSKA¹⁷, X. ZHANG²¹, X.L. ZHU²², S. ZWEBEN¹

Email: jberkery@pppl.gov

¹ Princeton Plasma Physics Laboratory, Princeton, NJ, United States of America

² University of Tennessee, Knoxville, TN, United States of America

³ Lehigh University, Bethlehem, PA, United States of America

⁴ General Atomics, San Diego, CA, United States of America

⁵ Massachusetts Institute of Technology, Cambridge, MA, United States of America

⁶ University of California at Los Angeles, Los Angeles, CA, United States of America

⁷ Commonwealth Fusion Systems, Devens, MA, United States of America

⁸ Institute for Plasma Research, Bhat, Gandhinagar, India

⁹ Princeton University, Princeton, NJ, United States of America

¹⁰ ITER Organization, St. Paul Lez Durance, France

¹¹ University of Texas at Austin, Austin, TX, United States of America

¹² Nova Photonics, Princeton, NJ, United States of America

¹³ Type One Energy, Madison, WI, United States of America

¹⁴ CompX, Del Mar, CA, United States of America

¹⁵ Seoul National University, Seoul, Republic of Korea

¹⁶ United Kingdom Atomic Energy Authority, Abingdon, United Kingdom

¹⁷ Columbia University, New York, NY, United States of America

¹⁸ University of Wisconsin, Madison, WI, United States of America

¹⁹ Lawrence Livermore National Laboratory, Livermore, CA, United States of America

²⁰ Oak Ridge National Laboratory, Oak Ridge, TN, United States of America

²¹ Tokamak Energy Ltd., Milton Park, United Kingdom

²² Dalian University of Technology, Dalian, China

Abstract

The objectives of NSTX-U research are to reinforce the advantages of STs while addressing the challenges. To extend confinement physics of low- A , high beta plasmas to lower collisionality levels, understanding of the transport mechanisms that set confinement performance and pedestal profiles is being advanced through gyrokinetic simulations, reduced model development, and comparison to NSTX experiment, as well as improved simulation of RF heating. To develop stable non-inductive scenarios needed for steady-state operation, various performance-limiting modes of instability were studied, including MHD, tearing modes, and energetic particle instabilities. Predictive tools were developed, covering disruptions, runaway electrons, equilibrium reconstruction, and control tools. To develop power and particle handling techniques to optimize plasma exhaust in high performance scenarios, innovative lithium-based solutions are being developed to handle the very high heat flux levels that the increased heating power and compact geometry of NSTX-U will produce, and will be seen in future STs. Predictive capabilities accounting for plasma phenomena, like edge harmonic oscillations, ELMs, and blobs, are being tested and improved. In these ways, NSTX-U researchers are advancing the physics understanding of ST plasmas to maximize the benefit that will be gained from further NSTX-U experiments and to increase confidence in projections to future devices.

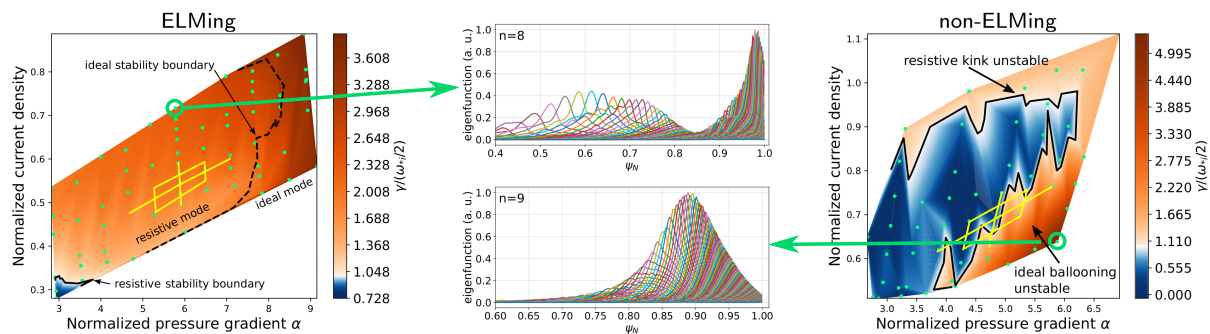


FIG. 1. Extended-MHD peeling-ballooning stability limits and normalized growth rates in NSTX are shown for an ELMing discharge (left) and non-ELMing discharge in wide-pedestal H-mode (right). ELMing discharges are unstable to resistive kink-peeling modes, and the ideal-MHD stability threshold is indicated by the dashed line. For non-ELMing cases the ideal and resistive stability boundaries are similar and experiments are located close to the ideal ballooning threshold. The unstable domain is shown in red, and the stable domain in blue. The center shows the poloidal spectrum of a typical resistive kink-peeling mode as found in ELMing cases (top) and of an ideal ballooning mode in the non-ELMing case (bottom).

1. INTRODUCTION

Spherical tokamak (ST) concepts are currently being designed for fusion pilot plants [1], both in the public and private sectors. The National Spherical Torus Experiment (NSTX) has historically provided much of the physics basis for the ST concept for fusion energy production. Researchers are now advancing the physics understanding of ST plasmas to maximize the benefit that will be gained when the upgraded device (NSTX-U [2]) returns to operation and to increase confidence in projections to future devices [3]. STs have certain advantages: their more compact size means they can provide higher plasma current more economically. Their low aspect ratio, A , improves stability with favorable average curvature, and high elongation also improves confinement and stability, enabling high β (the ratio of plasma pressure to magnetic pressure). There are challenges as well: managing the high heat flux, and start-up and sustainment of the plasma without space in the center column for an induction coil. The objectives of NSTX-U research are to reinforce the advantages while addressing the challenges: (i) to extend confinement physics of low- A , high beta plasmas to the lower collisionality levels relevant to burning plasma regimes, (ii) to develop stable, low-disruptivity, large bootstrap fraction, non-inductive scenarios needed for steady-state operation, and (iii) to develop power and particle handling techniques to optimize plasma exhaust in high performance scenarios.

2. EXTENDING CONFINEMENT PHYSICS OF LOW- A , HIGH BETA PLASMAS TO LOW COLLISIONALITY

Understanding of the transport mechanisms that set confinement performance and pedestal profiles is being advanced through gyrokinetic simulations, reduced model development, comparison to NSTX experiment (and forthcoming, lower collisionality NSTX-U experiments), as well as assessment of transport of energetic particles from neutral beam injection (NBI) or range of frequency (RF) heating.

2.1. Pedestal structure

Pedestal performance is a significant source of uncertainty in ST reactor design, and the pedestal properties of high confinement (H-mode) plasmas in NSTX have been seen to deviate from the standard model whereby ideal magnetohydrodynamic (MHD) peeling-ballooning macrostability limits the pedestal pressure and kinetic ballooning mode (KBM) microstability limits the pressure gradient.

A long-standing problem for ST pedestal stability prediction has been the reliable modeling of peeling-ballooning (P-B) stability boundaries. Unlike in large aspect ratio devices, ideal P-B modes are often predicted stable for ST discharges with unstable edge localized modes (ELMs). In simulations with the state of the art extended-MHD nonlinear M3D-C1 code [4], ELMing discharges in NSTX were seen to be limited by resistive current-driven peeling modes, with considerable sensitivity to plasma resistivity, whereas non-ELMing wide-pedestal discharges were located near the ideal pressure-driven ballooning threshold (see Fig. 1) [5]. Observations similar to the wide-pedestal H-mode have been made in enhanced-pedestal H-modes, i.e. these discharges are also limited by ideal pressure-driven modes. However, the linear stability picture is not as clear as for the other NSTX

discharges, as nonlinear stability is found to play a role in stabilizing in the non-ELMing nature of these plasmas. It is now being investigated whether the impact of resistivity on P-B stability is a result of spherical tokamak geometry (aspect ratio, shaping, etc.) or profile alterations due to lithium coating in NSTX. The model thus enables higher fidelity predictions for ELM thresholds and presents a valuable basis in the quest for a predictive model for ELMs in low-aspect ratio tokamaks.

Gyrokinetic analysis predicts that a variety of NSTX H-modes, from those with narrow pedestals and ELMs to wide ELM-free cases, are within 10% of KBM stability thresholds across the entire pedestal. This indicates KBM remains a viable candidate for constraining the maximum pressure gradient at low aspect ratio. Using gyrokinetic simulations to predict the onset of KBMs and other gyrokinetic instabilities, a new gyrokinetic linear threshold model reproduces the NSTX experimental width-height scaling (Fig. 2), which deviates significantly from standard aspect-ratio devices [6]. To predict NSTX(-U) and future ST pedestal width and height, the complimentary gyrokinetic KBM and resistive P-B stability constraints will be combined.

Progress is also being made towards pedestal transport validation and predictive modeling. The experimentally inferred ratio of electron particle to heat diffusivity (from the SOLPS code) is smaller than predicted by just KBM. This is consistent with the existence of both microtearing modes (MTM) and electron temperature gradient (ETG) modes, which are expected to transport primarily electron heat flux, and are predicted to be unstable. Nonlinear electron-scale ETG simulations predict a range of electron heat flux (0-2 MW) depending on local parameters. Combined with neo-classical (NC) ion thermal transport (~ 1 MW, from the NEO code), transport from ETG + NC accounts for 50-75% of the power flow for the wide pedestal and progressively less for the narrow pedestal. Nonlinear ion-scale MTM simulations predict electron heat flux comparable to that from ETG.

Together, ETG + MTM + NC accounts for the total power flow in a wide-pedestal discharge in which the largest deviations from KBM transport ratios are observed. To support evolution towards a predictive capability, additional simulations were used to develop a reduced ETG pedestal transport model that reproduces many of the dependencies with driving gradients and equilibrium parameters, unifying the NSTX results with those from recently published analysis from the higher aspect ratio DIII-D tokamak [7]. The results of this reduced model are shown in Fig. 3.

Linear gyrokinetics predicts that MTMs become dominant over ITG as the density is increased near the pedestal region and are predicted to be the dominant instability in the core in H-mode plasmas at similar densities (normalized to the Greenwald density) between NSTX(-U) and DIII-D [8]. This underscores the importance of considering the density in applications of MTMs to STs.

2.2. Core transport

Global confinement in NSTX H-modes has been observed to have scalings distinct from those in conventional aspect ratio devices. Thermal transport of core ions is typically found to be neoclassical in NSTX, while electron thermal losses dominate. Various gyrokinetic studies have been performed to explain this phenomenology. For high-beta NSTX discharges and NSTX-U projections that span over an order

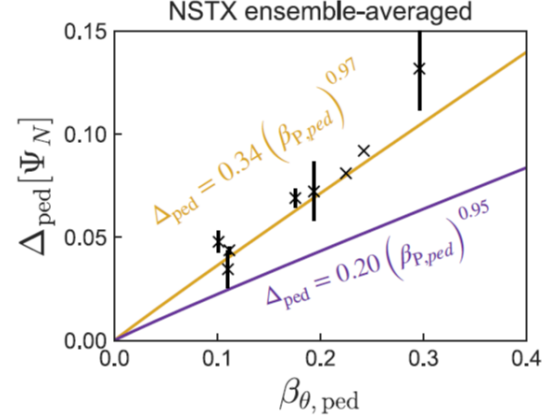


FIG. 2. Pedestal width in Ψ_N , Δ_{ped} , vs. pedestal height in β for various experimental NSTX discharges. The ideal ballooning critical pedestal prediction (purple) falls short of predicting the width, while the new gyrokinetic critical pedestal prediction matches the data.

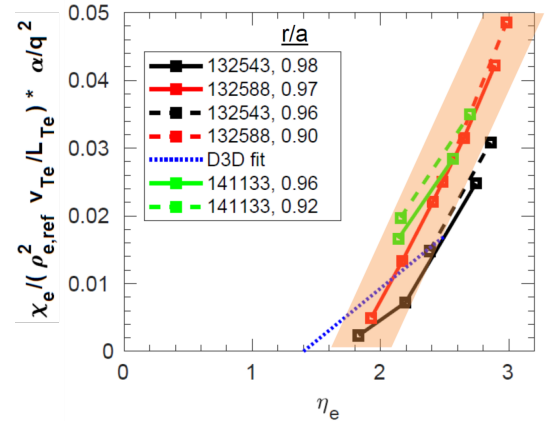


FIG. 3. A threshold-based reduced model for ETG transport shows overlap between NSTX and DIII-D simulations when α/q^2 , which goes like local equilibrium pressure gradient, is accounted for in plotting the gyroBohm-scaling-normalized ETG diffusion coefficient vs. the ETG drive, η_e , the ratio of density and temperature scale lengths.

of magnitude variation in collisionality, linear gyrokinetic simulations of ion-gyroradius-scale micro-instabilities show a complex mix of MTMs, trapped electron modes (TEMs), and hybrid TEM/KBM modes. Ion temperature gradient (ITG) instabilities, however, are typically stable in the NSTX discharges.

In most cases, simulations with CGYRO showed that modes that can produce ion transport were found to have growth rates smaller than the flow shear rate or thresholds much higher than the experimental NSTX gradients, consistent with the observed neoclassical ion thermal transport [9]. The analysis suggests ITG instabilities are unlikely to contribute significant anomalous thermal losses in high-beta, lower collisionality NSTX-U scenarios, and that KBMs are likely to play a role limiting the confinement by sitting near the threshold in most cases (see Fig. 4). Another CGYRO scan of aspect ratio and elongation found that while ETG or ITG were dominant for DIII-D, MTMs dominate in the NSTX range of parameters. Additionally, the high elongation and triangularity shaping capabilities of STs have also been shown, with the XGC code, to reduce the linear growth rates of both MTMs and KBMs [10].

Meanwhile, nonlinear global gyrokinetic simulations of MTMs with the GTS code are being carried out for experimental NSTX plasmas. As in previous local simulations, electron heat transport was found to be dominant, but additionally it was found that the $q = 1$ surface can play the role of transport barrier as turbulence propagates radially both inward, and equilibrium $E \times B$ sheared flow (electric field crossed with magnetic field), while stabilizing MTM, was found to possibly destabilize an Alfvénic Kelvin-Helmholtz instability. Equilibrium $E \times B$ sheared flows have sometimes been found to significantly suppress electrostatic ion scale transport in both gyrokinetic simulations and in experiment. For an NSTX case it was found that for sufficiently large magnetic shear, the $E \times B$ sheared flow acts to move modes through the ballooning angle, resulting in mode suppression. Nonlinear simulations using CGYRO found the MTM heat fluxes were suppressed when including $E \times B$ sheared flows matching experimental heat diffusivities.

Gyrokinetic theory, while an excellent approach to properly describe the microturbulent transport, is computationally expensive, so reduced models are critical to achieve real time profile predictions. However, these models must be validated against gyrokinetic simulations; several efforts are proceeding.

Turbulent and neoclassical heat transport have been calculated for NSTX with the flux-matching TGYRO (TGLF + NEO) solver, predicting experimental ion and electron temperature profiles. For a low confinement (L-mode) plasma, linear stability analysis and scans of temperature gradients identified the low- k and high- k unstable modes driving the turbulent electron and ion heat transport at the outer core region $\rho > 0.4$, where k is the wavenumber and ρ is the square root of normalized toroidal flux. In an H-mode plasma ETG modes drive the turbulent electron heat transport while the low- k modes are suppressed and the ion heat transport is predominantly neoclassical. Comparison with linear gyrokinetic stability analysis shows close agreement of the real frequencies of unstable modes between TGLF and CGYRO gyrokinetic simulations, but higher growth rates are predicted by TGLF, especially for the H-mode case.

An improvement in understanding of electron thermal transport is made possible by using a Multi-Mode-Model (MMM) of anomalous transport, which includes a new physics-based electron temperature gradient (ETG) model [11] as well as an upgraded

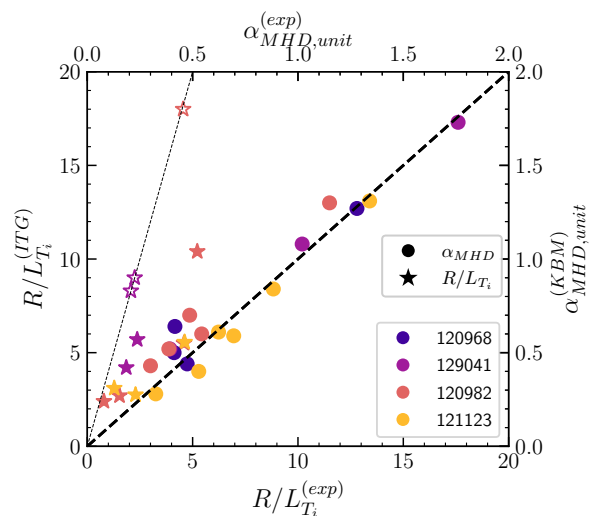


FIG. 4. Summary of ITG thresholds (R/L_{T_i} , on bottom and left axes) and KBM thresholds ($\alpha_{MHD,unit}^{(KBM)}$, on top and right axes) calculated with gyrokinetic (CGYRO) simulations against the corresponding experimental value, combining different discharges and radial positions (from $0.4 < r/a < 0.8$). For the ITG case, the open stars indicate that the R/L_{T_i} gradient was increased four times without finding any threshold.

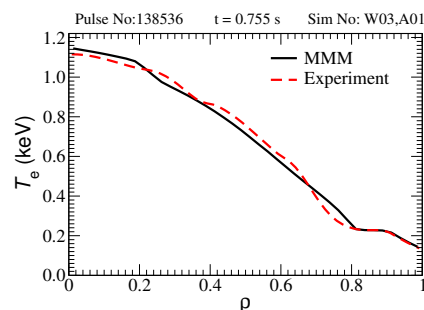


FIG. 5. MMM-simulated (black) and TRANSP-processed experimental (red) electron temperature profiles for the low collisionality NSTX discharge 138536 ($t = 0.75$ s).

MTM model. The ETG model has been verified through its comparison with CGYRO simulations. The magnitude and associated real frequency of the most unstable ETG mode present in the $k_y \rho_s$ spectrum agree with the results obtained from CGYRO. The MMM model reproduces the experimentally measured thermal power of 2.0 MW and produces electron temperature profiles that are consistent with the NSTX experimental data in a low collisionality discharge where ETG diffusivity is larger than MTM, as shown in Fig. 5.

CGYRO was used to study linear and nonlinear ETG modes in NSTX(/-U) and compared with reduced ETG models to better determine their applicability. Linear simulations determine the ETG critical gradient, contrasting it with the standard tokamak scaling formula. This formula appears insufficient to describe the threshold when applied to STs. Within the deep core ($r/a < 0.3$), where the normalized temperature gradient is typically less than the experimental value, no ETGs manifest. In the transport region ($r/a \sim 0.6 - 0.8$), ETG stability varies across cases. Nonlinear simulations that calculate electron thermal transport align well with NSTX experimental data within uncertainties. Furthermore, the reduced model ETGM [11], displaying strong agreement with experimental measurement and CGYRO simulations, instills confidence in its utility for profile prediction in future NSTX-U discharges.

2.3. Impurity transport

Besides transport of main ion species and electrons, transport of impurities and energetic ions is also important to understand. Resonant magnetic perturbations (RMPs) are sometimes applied in tokamaks to suppress ELMs. However, RMPs often result in a decrease in the plasma density, also termed density-pumpout. The role of neoclassical transport in density-pumpout can be analyzed by using a coupling of the M3D-C1 and 3D-NEO codes [12]. The neoclassical fluxes of impurities evaluated for the NSTX discharge 130670 shows that, if an impurity resides in the low collisionality regime it will experience significant changes in 3D perturbed flux with RMPs (compared to the axisymmetric flux), but is weakly affected by RMPs in the Pfirsch-Schlüter regime. Since the atomic number (Z) of impurity species affects the collisionality, the transport of low- Z impurities is greatly altered with RMPs but has a smaller effect for higher Z impurities.

2.4. RF Heating

Simulation capabilities for RF heating are expanding greatly in general. The use of the Petra-M finite element method platform allowed for simulations with very high-fidelity for the first time of the full 3D NSTX-U torus including realistic antenna geometry in the high harmonic fast wave (HHFW) heating regime [13]. More recently, RF sheath effects have also been implemented in Petra-M [14]. RF sheaths can form during ion cyclotron RF operation and contaminate the plasma with impurities [14], so it is very important to have a quantitative analysis for the future NSTX-U HHFW experimental campaign. Finally, a numerical study of the impact of the edge density fluctuations and filaments on the HHFW wave propagation have been recently started as well [15]. In fact, resonant wave-filament interactions have been shown to be a loss mechanism for HHFW power [16] and can explain the large fraction of RF power flows along the field lines in NSTX that hit the divertor, rather than heating the core plasma [17].

A large percent of HHFW injected power can be lost in the plasma boundary on NSTX. New 1D particle-in-cell simulations are conducted to investigate a possible role of parametric decay instabilities (PDI). The PDI excitation has been identified near the lower hybrid resonance layer where the thermal effects becomes non-negligible, and can form a power loss channel. The modeling also suggests that parasitic electrostatic wave excitation, such as Ion Bernstein waves and hot ion plasma waves, can lead to anisotropic perpendicular ion heating, in line with the previous ion temperature measurement on NSTX during HHFW experiments. When this resonance layer is removed in the simulation domain by raising the density, PDIs are suppressed despite a large increase in the input power, indicating that a presence of the lower hybrid resonance density layer can be a key parameter in determining the convective growth.

Machine learning based surrogate models are being employed to accelerate RF modeling codes. In particular, fast and accurate HHFW predictions in NSTX/NSTX-U have been obtained via training surrogates on full-wave solutions. The achieved average inference times on the order of microseconds are necessary to incorporate an HHFW model into integrated frameworks for both time-dependent simulations and real-time control applications.

Finally, transport of energetic particles (EPs) can be complicated when multiple sources of these particles are simultaneously employed, for example by neutral beam injection (NBI) and RF heating. Modifications of the NBI distribution on NSTX(/-U) as RF was added to the simulations was assessed with the ORBIT code, where increased losses of NB ions that are displaced to loss orbits by the RF field were found. The modified NBI distribution can subsequently have an effect on Alfvénic instabilities, either stabilizing or destabilizing, depending on how the RF tail distribution aligns and overlaps with Alfvén eigenmode resonances in the EP phase space.

3. DEVELOPING STABLE, LOW-DISRUPTIVITY, LARGE BOOTSTRAP FRACTION, NON-INDUCTIVE SCENARIOS FOR STEADY-STATE OPERATION

In order to achieve high performance discharges in NSTX-U and project low disruptivity operation to future steady state STs, various performance-limiting modes of instability were studied and predictive tools were developed.

3.1. Stability: Low-frequency modes, tearing modes, and islands

One performance-limiting mechanism in NSTX was that the central electron temperature tended to remain largely unchanged as the external heating power increased above a certain level. Various explanations have been proposed for this behavior, including Alfvén eigenmodes either directly influencing electron thermal transport, or modifying the power deposition from neutral beams. Resistive 3D MHD simulations with M3D-C1 have now shown another possible explanation, that low toroidal mode number n , pressure-driven ideal MHD instabilities, though non-disruptive, acted to break magnetic surfaces in the plasma core, thereby flattening the electron temperature profiles above a critical beta value [18, 19]. Accounting for this effect for future devices may project somewhat lower performance, but it may be a more accurate prediction, and also motivates studies to potentially avoid these modes.

As described, electron thermal transport in NSTX was routinely characterized as anomalous. Operating with reversed magnetic shear (RMS) was shown to suppress the anomalous transport through the development of electron internal transport barriers when the shear was sufficiently negative. By utilizing TRANSP, RMS operating scenarios were developed in NSTX-U. It was found that procedures similar to those used in NSTX can be followed in NSTX-U to establish RMS. This includes creating as large a plasma as possible with a fast current ramp and early neutral beam injection to heat electrons and slow the current diffusion for the edge to the core. Additionally, all such scenarios have shear levels beyond the threshold found in NSTX for transport suppression. Early reversed shear profiles above $q_0 = 1$ are potentially prone to resistive MHD instabilities known as double tearing modes, however. An example of such a mode from NSTX has now been investigated with M3D-C1, where it was found that sometimes these modes can lead to flux-surface breakup that may persist throughout the discharge.

The evolution of the q profile was key to performance in other ways as well. Low frequency (< 50 kHz) MHD $n = 1$ and 2 mode activity was often present in the first 400 ms of NSTX discharges and may have inhibited even higher performance. Observations of these modes in relation to the equilibrium evolution, and a 3D study with M3D-C1 showed that they formed in the core when the safety factor at the magnetic axis, q_0 , reached a mode rational value, and then slowly moved outwards with the mode rational surface while remaining locked to the core, flattening the core T_e and rotation profiles. When the rational surface moved sufficiently far from the core, the core would unlock from the mode. When the q_0 evolution is fast enough to cross multiple rational surfaces before the core unlocks from the early mode, a characteristic “bifurcation” in the magnetic spectrogram can be observed. This understanding of these modes is the first step towards either avoiding them to increase performance, or at least maintaining a current evolution that allows the plasma to push through these early modes [20].

Magnetic islands and tearing modes can continue to affect the steady-state plasma. Steady state operation in future ST devices will require fully non-inductive current, but simulations have shown that for large aspect ratio devices, a significant reduction of bootstrap current over large radial extent is attributable to magnetic islands. A gyrokinetic study of the effect of MHD islands on self-driven current in NSTX has now shown, however, that though tearing modes (and islands) are more prominent in high poloidal β regimes, the bootstrap current reduction is less sensitive to island width in this regime, and is therefore much less significant in STs [21]. Still, it is important to model the growth of magnetic islands and triggered or triggerless neoclassical tearing modes (NTMs). First, NTMs could be triggered by resonant magnetic perturbations (RMPs) in NSTX, and a theoretical simulation of that process showed that in the presence of a frequency mismatch between the rotation frequency of seed island and that of the RMP, the critical RMP amplitude needed to trigger an RMP oscillates as the duration of the RMP pulse is varied [22]. The critical amplitude is minimized when the RMP pulse duration is such that seed island chain executes a half-integer number of rotations with respect to the pulse. Tearing modes may also be triggered by a sawtooth instability, which induces loss of EPs. An improved model of EP transport by sawteeth has now been implemented for TRANSP. Contrary to previous models already implemented in TRANSP, the new model resolves EP transport in phase space based on the workflow implemented for the “kick model”. The model has been tested on NSTX-U [23], and it will enable a better quantitative understanding and prediction of plasma discharges. Finally, a model was developed using the TRANSP code to calculate the parameters of the modified Rutherford equation to predict the growth of magnetic islands [24]. An application of the model to the triggerless neoclassical tearing modes (NTMs) observed in NSTX showed that the model prediction agrees with the measurement when the energetic particle (EP) term is added to the modified Rutherford equation. The TRANSP “kick” model is used to calculate the input EP pressure and density profile self consistently, with the EP transport due to magnetic islands considered.

3.2. Energetic particle stability

Non-resonant $n = 1$ fishbone modes driven by EPs in plasmas with q_{min} slightly larger than one can lead to degradation of plasma confinement. These modes were studied with M3D-C1 by extending the code to include kinetic effects of both thermal ions and energetic ions, and the perturbation on magnetic flux surfaces as well as the transport of energetic particles can be calculated [25]. It was found that the thermal ion kinetic effects can cause an increase of the frequencies of the modes, and that Landau damping can provide an additional stabilization effect [26].

A method of analytic predictive fast ion transport modeling has been extended to NSTX-U regimes. Unlike in conventional tokamaks, the fast ion effective dynamical friction (drag) rate in STs is typically of the same order of the fast ion effective scattering rate. A new theoretical formulation [27] for marginally unstable modes has reported that in those scenarios, resonances of Alfvénic eigenmodes tend to shift and split their most active regions of energy exchange with the fast ion sub-population, thereby effectively extending the instability drive range. Mode saturation levels within that reduced analytical framework have been shown to lead to the exact same levels as fully nonlinear kinetic theory. This analytic extension allows for a self-consistent, fully predictive and numerically efficient fast ion transport module through the Resonance-Broadened Quasilinear (RBQ) code.

Toroidal Alfvén eigenmode (TAE) avalanches in NSTX were always accompanied by simultaneous rapid frequency-chirping and large amplitude bursting of multiple modes, and the avalanches led to significant energetic particle losses. The experimental phenomenon has now been reproduced by non-linear, multiple wave number simulation results, which identified wave-wave nonlinear coupling among different modes as an important ingredient for the onset of TAE avalanches, during which there is a resonant interaction between different modes and energetic particles [28]. One of the distinctive features of TAEs excited in NSTX and other spherical tokamaks is the rapid down-chirping of mode frequency after saturation. Using M3D-C1, this post-saturation frequency decrease has now been effectively replicated in nonlinear simulations. The chirping rate was found to be closely related to the continuum damping of the TAEs and the shear of the toroidal rotation. In the nonlinear stage, a substantial portion of EPs can be transported from the core to the outer region. This transport leads to increased interaction with the perturbed fields of the mode, resulting in a further amplification of the mode.

Finally, Global Alfvén eigenmodes (GAEs) in NSTX driven by energetic particles have been linked to enhanced electron transport and may be expected to affect the performance of NSTX-U and future STs where super-Alfvénic fast ions might be present. Studies of the amplitude and phase of bursts of GAEs in NSTX indicate that the first harmonic can non-linearly drive weakly damped modes in the second harmonic frequency band [29]. It is further seen that these short wavelength Alfvénic modes can be strongly toroidally localized. Fully nonlinear simulations of the evolution of unstable GAEs in NSTX-U demonstrate the importance of including all toroidal harmonics for accurate prediction of saturation amplitudes, and show a significant redistribution of resonant fast ions and modification of the beam distribution even by relatively small amplitude modes [30].

3.3. Disruptions and machine protection

The Disruption Event Characterization and Forecasting (DECAFTM) NSTX-U 2016 database for vertical displacement events (VDE), plasma current not meeting the request (IPR), disruptive current spike (DCS), or current quench start (CQS). VDE and DCS are prominent at the high κ and l_i boundary.

The Disruption Event Characterization and Forecasting (DECAFTM) NSTX-U 2016 database was developed to understand the chains of events leading to disruption in many machines, including NSTX(-U); examples of DECAF physics modules include the following. First, standardization of the determination of disruption timing between machines will allow comparable analysis of multi-machine databases, and DECAF has now been updated to utilize abnormal plasma current and vertical position signals to accomplish this [32]. An example DECAF analysis of the NSTX-U 2016 database is shown in Fig. 6. Second, vertical stability detection approaches have themselves been compared between real-time reconstructions and magnetic probe measurements, resulting in critical metrics and thresholds for predicting vertical displacement events. Third, automatic detection of H to L-mode back transitions based on electron temperature, T_e , deuterium-alpha radiation, D_α , stored energy, and energy confinement time signals has been implemented to study the correlation and causality of confinement back transitions with disruptions. Fourth, the novel technique of counterfactuals was used to assess hypothetical MHD activity or normalized β levels that would have

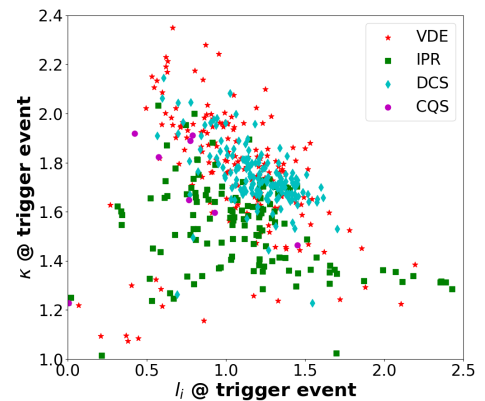


FIG. 6. Elongation vs. internal inductance at the disruption trigger event time for the NSTX-U 2016 database for vertical displacement events (VDE), plasma current not meeting the request (IPR), disruptive current spike (DCS), or current quench start (CQS). VDE and DCS are prominent at the high κ and l_i boundary.

prevented resistive wall modes from going unstable in experimentally unstable discharges, motivating the usage of the counterfactual technique to simulate real-time control [33]. Finally, the physics of the density limit has been recently explored theoretically through local phenomenon, such as power balance at magnetic islands or turbulent transport at the plasma boundary. The former has been tested as a disruption indicator in NSTX-U discharges [31, 34], but so far was not found to be as reliable as the Greenwald limit. The latter was tested vs. some MAST-U discharges and found to be potentially useful for spherical tokamak disruption prediction [34].

Runaway electron (RE) generation presents a possibly large issue for future devices due to the potential for damage to the structures. In tokamaks RE can be generated after disruptions but also during the early stages of the discharge start-up, when higher electric fields are needed to increase the current through cold plasmas. NSTX contributed unique low aspect ratio data to a multi-machine database for RE generation and confinement during startup [35]. The multi-machine comparison demonstrated that the thermalization of the startup REs and the suppression of secondary generation of REs is sensitive to the dynamics of the density, the electric field and thus also the temperature during the start-up phase. Data from NSTX at a low aspect ratio was critical for demonstrating the drift-orbit losses of REs are not the primary loss mechanism for startup REs [35].

3.4. Equilibrium reconstruction, integrated modeling, and control

Tools are being developed for NSTX-U for fast prediction and optimization of plasma scenarios, including neural networks trained on the EFIT equilibrium reconstruction code as well as prediction of non-rigid plasma response for shape control [36]. These can be used in forward-mode for simulation of plasma scenarios before they are run, or reconstruction mode for real-time equilibrium reconstruction, and have shown some performance improvements over the existing real-time EFIT.

The OMFIT integrated modeling workflow has been set up for NSTX and NSTX-U, including obtaining the full kinetic equilibrium reconstruction with EFIT-AI, analysis of power balance fluxes, and prediction of heat plasma profiles based on a reduced turbulence model. The integrated workflow addresses tasks of kinetic profiles fitting integrated with the transport code TRANSP and EFIT to provide a self-consistent equilibrium reconstruction with kinetic constraints of total pressure, including beam pressure, and total current, including bootstrap current. GSevolve, a free boundary equilibrium that evolves the Grad-Shafranov equilibrium including current and pressure profiles, will be connected to the NSTX-U plasma control system. GSevolve simulations can improve NSTX-U control and performance by, for example, stably controlling and increasing elongation in the plasma current rampup. NSTX-U discharges with vertical displacement events have been simulated successfully as well as from breakdown to termination. The inclusion of high resolution current profile simulation provides a close match to interpretative experimental analysis from TRANSP.

Tight simultaneous regulation of several plasma parameters, both scalars and profiles, during the tokamak discharge is important for maintaining steady-state, non-disruptive scenarios. Feedforward+feedback controllers based on both off-line and on-line optimization are being designed for plasma-scenario regulation in NSTX-U. A Linear Quadratic Integral (LQI) regulator has been synthesized for simultaneous regulation of the q profile and normalized beta β_N [37], while a Model Predictive Controller (MPC) has been developed for simultaneous control of multiple scalar quantities, including q_0 , β_N , and internal inductance. Moreover, a hybrid MPC for dual q -profile and stored energy regulation has been proposed to explicitly incorporate the pulse-width-modulation constraints imposed by the NSTX-U NBI system. Finally, a method of significantly reducing the computational time of a model-based feedforward-control optimization scheme for q -profile shaping in NSTX-U has also been devised, whereby analytical cost function gradients are used in place of numerical gradients in order to ensure a faster convergence to the optimized actuator trajectories [38].

4. DEVELOPING POWER AND PARTICLE HANDLING TECHNIQUES TO OPTIMIZE PLASMA EXHAUST IN HIGH PERFORMANCE SCENARIOS

The increased heating power and compact geometry of NSTX-U will produce very high heat flux levels that will be seen in future high performance STs as well. Innovative solutions to handle these heat fluxes and predictive capabilities accounting for plasma phenomena must be developed, tested, and improved.

4.1. Lithium

The NSTX(-U) program of research has pioneered the study of lithium as a renewable surface at the plasma-material interface that protects the underlying solid substrate, improves confinement through particle pumping, and enhances power exhaust capability, including heat flux redistribution due to vapor shielding from evaporated lithium.

The fact that NSTX-U can produce very high heat fluxes makes it an excellent candidate for a future test facility for lithium divertor solutions. One such solution is to dissipate the heat flux in a simple configuration called a lithium vapor box (LVB) that evaporates lithium in the private flux region. Divertor detachment is desired to protect plasma facing components (PFCs), but can create a highly radiating X-point and upstream ionization could lead to non-negligible lithium content, so a LVB baffled design has been studied with the SOLPS-ITER code using an NSTX-U magnetic equilibrium. Private flux region gas puffing was shown to reduce the upstream lithium contamination significantly more than common flux region puffing due to better access to the separatrix [39] (Fig. 7).

Lithium flows primarily along the separatrix due to the hotter field line having a stronger thermal force which pushes the lithium upstream. The effect of the fuel puff for a given intensity depends strongly on the recycling coefficients assumed for the various plasma facing components in the simulation. Additionally, many lithium vapor-shielding high-density divertor concepts rely on non-coronal lithium radiation that can be affected by radiation transport. Work is now underway to clarify the role of lithium radiation transport on radiated power and charge state distribution in these divertors [40]. Test stand experiments of lithium vapor boxes are being implemented, and such a concept could be considered for future use on NSTX-U.

Another approach is to place liquid lithium directly at the strike point. In one such design, a porous wall is used to stabilize the liquid metal surface, while an MHD drive is used to push the liquid metal flow underneath the porous surface. This same concept has now also been optimized to work as an evaporating surface for the LVB. Analytical and numerical models for liquid lithium plasma facing components (PFCs) [41] allow parametric studies of the design variants and optimization, as well as detailed mapping of the flow and heat transfer distributions. The plasma heat flux distribution is obtained using SOLPS analysis, while numerical simulation of the PFCs uses a version of the 3D computational fluid dynamics code CFX from ANSYS. It can predict the temperature distribution on the liquid metal plasma facing component, in different design conditions. The resulting distribution can then be used to establish a two-way coupling between an analytical model and SOLPS. The code was modified to simulate MHD flows at high Hartmann numbers. Finally, the optimized design of the flowing liquid lithium device with porous walls has now been used to create conceptual replacement tiles for the NSTX-U divertor.

Many challenges remain for lithium solutions to be viable for fusion reactors, but the liquid lithium program in NSTX-U is geared to close some of the gaps, and the designs are coupled to reactor designs of liquid lithium PFCs [42].

4.2. Divertor heat flux

Heat fluxes on NSTX-U solid PFCs (divertor tiles) have previously been analyzed in 3D and with time variation with the HEAT code. The code has now been updated with an ion-gyro orbit module, and the gyro-orbit effects were shown to alternately enhance PFC performance by smearing magnetic shadows and degrade performance when narrow regions on edges and corners are loaded with high heat fluxes [43].

A reduced model for scrape-off layer plasma transport was developed and tested against NSTX(/-U) experimental observations and high fidelity interpretive simulations [44]. The model addresses core-edge physics problems such as edge ionization sources and neutral densities by coupling to the kinetic neutral transport code DEGAS2, and fast ion confinement with a novel numerical algorithm for integrating the stochastic differential equation for pitch angle scattering. The model can additionally use Langmuir probe data to reconstruct the calculation of the upstream density and electron temperature and can be used in TRANSP to constrain recycling coefficients, thereby providing an efficient and fast coupling between core and edge to support experimental planning and discharge scenario development.

Other plasma phenomena can influence heat flux as well, and it is important to understand these to accurately predict the performance of PFCs for NSTX-U, where the predictions can be tested and then confidently projected to future, higher power STs. One of these phenomena is the edge harmonic oscillation (EHO), which was analyzed and found to be beneficial by decreasing the divertor peak heat flux when background edge fluctuations were low, and increasing the heat flux width (more with larger EHO frequency) [45]. However, when background edge fluctuation levels were high, the EHO was found to increase the divertor peak heat flux. The divertor peak heat flux decreases with the frequency of EHO $n = 1$ mode, while the heat flux width increases with the frequency of

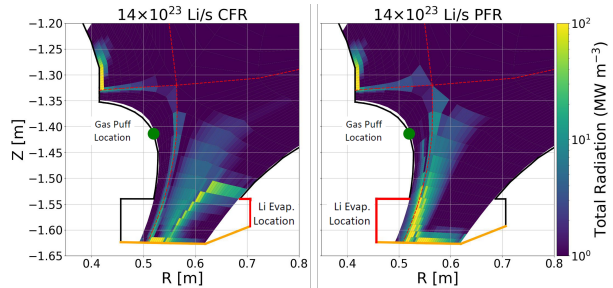


FIG. 7. Differences in the radiation distribution between common flux region (left) and private flux region (right) evaporation of lithium in a lithium vapor box design for NSTX-U.

the EHO $n = 1$ mode.

High plasma edge turbulence in NSTX H-modes was found to significantly increase the divertor heat flux width to levels comparable with the divertor heat flux in L mode, and possibly up to three times larger than the multi-machine scaling results [46]. Edge localized modes (ELMs) may cause problems for future STs by releasing bursts of energy from the plasma, but they were found in NSTX to cause heat flux striations that were beneficial (to the divertor, at least) by significantly increasing the heat flux width and decreasing the divertor peak heat flux during the ELMing period vs. the inter-ELM period, also to levels similar to L-mode. A characteristic signature for the effect of small ELMs on the lower outer divertor heat flux is in NSTX is shown in Fig. 8. The ELMs were observed from the D_α signal on the lower divertor in Fig. 8(b) and the deposited power (P_{div}) on the lower divertor is shown in Fig. 8(c). After the L-H transition at ~ 0.153 s (red dashed line), the divertor heat flux shrunk, which caused the q_{peak} to increase from 1.2 MW/m² to ~ 3.5 MW/m². After 0.22 s the ELMs appear, and the P_{div} increased by $< 50\%$ with small ELMs. However, q_{peak} significantly decreased from 3 MW/m² (ELM free), to < 1.5 MW/m² (small ELMs), as shown in Fig. 8(d). The divertor peak heat flux during these small ELMs had a similar level to L-mode discharges.

4.3. Blobs

ELM filaments transport energy and particles out of the confined plasma region to the scrape-off layer and eventually to the plasma facing components. These structures are similar to the intermittent ‘‘blobs’’ appearing in the background SOL turbulence. Gas-puff imaging data from NSTX has been analyzed and while ELM filaments and blobs were found to be of similar size and shape, the ELM filaments internally rotated about three times faster and the angular velocity increased with the distance from the separatrix [47]. Novel data analysis techniques were needed to be developed to assess the angular velocity on a frame-by-frame time resolution [48]. The understanding of filamentary dynamics is important to develop the ability to predict and mitigate the impact of ELMs on plasma facing components. The blobs were also studied and in NSTX were shown to decrease in quantity with NBI power, be less prevalent in H-mode than L-mode, and depend most strongly on the poloidal turbulence velocity [49]. Temporally, blobs came in pulses that lasted on the order of $25 \mu\text{s}$, while the wait time between pulses was typically about 1 ms [50]. A theory for the mechanism of blob formation based on velocity shear breaking radially elongated streamers was satisfactorily tested against NSTX data [51].

ACKNOWLEDGEMENTS

This work was supported by the U.S. Department of Energy under contract numbers DE-AC02-09CH11466 (PPPL), DE-AC02-05CH11231 (NERSC resources), DE-SC0008309 (UT, Knoxville), DE-SC0013977 (Lehigh), DE-SC0021385 (Lehigh), DE-SC0021113 (GA), DE-FG02-95ER54309 (GA), DE-FG02-91ER54109 (MIT), DE-SC0021156 (UT, Austin), DE-SC0021625 (Nova Photonics), DE-SC0021311 (Columbia), DE-AC52-07NA27344 (LLNL), and the early career research program. Additionally: EP/R034737/1 (UKAEA).

The United States Government retains a non-exclusive, paid-up, irrevocable, world-wide license to publish or reproduce the published form of this manuscript, or allow others to do so, for United States Government purposes.

REFERENCES

- [1] MENARD, J.E. ‘‘Next-step low-aspect-ratio tokamak design studies’’. IAEA Fusion Energy Conference (London, UK, 2023). P/8 2215.

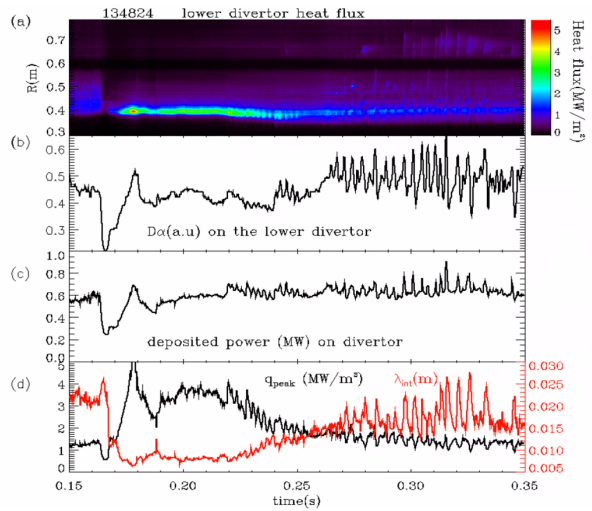


FIG. 8. NSTX discharge 134824 with small ELMs: (a) contour plot of the heat flux profile as a function of radius and time, (b) the evolution of the D_α on the lower divertor (c) the evolution of the deposited power on lower divertor and (d) the evolution of integral heat flux width (λ_{int}) and divertor heat flux width (q_{peak}).

- [2] MICHELETTI, D. “NSTX-U recovery project status and plans”. IAEA Fusion Energy Conference (London, UK, 2023). P/1 1624.
- [3] GUTTENFELDER, W. et al. “NSTX-U theory, modeling and analysis results”. *Nucl. Fusion* 62.4 (2022), p. 042023.
- [4] FERRARO, N.M. “The M3D-C1 code as a tool for design validation and whole-device modeling”. IAEA Fusion Energy Conference (London, UK, 2023). P/3 2151.
- [5] KLEINER, A. et al. “Critical role of current-driven instabilities for ELMs in NSTX”. *Nucl. Fusion* 62.7 (2022), p. 076018.
- [6] PARISI, J. “A gyrokinetics-based model for predicting pedestal width scaling at arbitrary aspect ratio”. IAEA Fusion Energy Conference (London, UK, 2023). TH/3 2325.
- [7] GUTTENFELDER, W. et al. “Testing predictions of electron scale turbulent pedestal transport in two DIII-D ELMy H-modes”. *Nucl. Fusion* 61.5 (2021), p. 056005.
- [8] McCLENAGHAN, J. et al. “Transition from ITG to MTM linear instabilities near pedestals of high density plasmas”. *Phys. Plasmas* 30.4 (2023), p. 042512.
- [9] CLAUSER, C.F. et al. “Linear ion-scale microstability analysis of high and low-collisionality NSTX discharges and NSTX-U projections”. *Phys. Plasmas* 29.10 (2022), p. 102303.
- [10] SHARMA, A.Y. et al. “Global gyrokinetic study of shaping effects on electromagnetic modes at NSTX aspect ratio with ad hoc parallel magnetic perturbation effects”. *Phys. Plasmas* 29.11 (2022), p. 112503.
- [11] RAFIQ, T. et al. “Electron temperature gradient driven transport model for tokamak plasmas”. *Phys. Plasmas* 29.9 (2022), p. 092503.
- [12] SINHA, P., FERRARO, N.M., and BELLI, E. “Neoclassical transport due to resonant magnetic perturbations in DIII-D”. *Nucl. Fusion* 62.12 (2022), p. 126028.
- [13] BERTELLI, N., SHIRAIWA, S., and ONO, M. “3D full wave fast wave modeling with realistic HHFW antenna geometry and SOL plasma in NSTX-U”. *Nucl. Fusion* 62.12 (2022), p. 126046.
- [14] SHIRAIWA, S. et al. “Magnetic potential based formulation for linear and non-linear 3D RF sheath simulation”. *Nucl. Fusion* 63.2 (2023), p. 026024.
- [15] BERTELLI, N. “A detailed study of the interaction between the high harmonic fast wave and the scrape-off layer region in NSTX/NSTX-U plasmas”. IAEA Fusion Energy Conference (London, UK, 2023). P/3 1841.
- [16] TIERENS, W. et al. “Resonant wave–filament interactions as a loss mechanism for HHFW heating and current drive”. *Plasma Phys. Control. Fusion* 64.3 (2022), p. 035001.
- [17] TIERENS, W. et al. “On the origin of high harmonic fast wave edge losses in NSTX”. *Nucl. Fusion* 62.9 (2022), p. 096011.
- [18] JARDIN, S.C. et al. “Ideal MHD limited electron temperature in spherical tokamaks”. *Phys. Rev. Lett.* 128 (24 2022), p. 245001.
- [19] JARDIN, S.C. et al. “Ideal MHD induced temperature flattening in spherical tokamaks”. *Phys. Plasmas* 30.4 (2023), p. 042507.
- [20] MUNARETTO, S., FERRARO, N. M., and FREDRICKSON, E. D. “On the frequency bifurcations of the MHD startup modes in NSTX”. *Phys. Plasmas* 30.6 (2023), p. 062502.
- [21] WANG, W. “Reduction of plasma self-driven current by magnetic island perturbations in tokamaks”. IAEA Fusion Energy Conference (London, UK, 2023). P/4 2313.
- [22] FITZPATRICK, R. et al. “Theoretical investigation of the triggering of neoclassical tearing modes by transient resonant magnetic perturbations in NSTX”. *Phys. Plasmas* 30.7 (2023), p. 072505.
- [23] PODESTÀ, M. et al. “Development of a reduced model for energetic particle transport by sawteeth in tokamaks”. *Plasma Phys. Control. Fusion* 64.2 (2022), p. 025002.
- [24] YANG, J. et al. “Nonlinear growth of magnetic islands by passing fast ions in NSTX”. *Plasma Phys. Control. Fusion* 64.9 (2022), p. 095005.
- [25] LIU, C. et al. “Hybrid simulation of energetic particles interacting with magnetohydrodynamics using a slow manifold algorithm and GPU acceleration”. *Comput. Phys. Commun.* 275 (2022), p. 108313.
- [26] LIU, C. et al. “Thermal ion kinetic effects and Landau damping in fishbone modes”. *J. Plasma Phys.* 88.6 (2022), p. 905880610.

- [27] DUARTE, V.N. et al. “Shifting and splitting of resonance lines due to dynamical friction in plasmas”. *Phys. Rev. Lett.* 130 (10 2023), p. 105101.
- [28] ZHU, X.L. et al. “Avalanche transport of energetic-ions in magnetic confinement plasmas: nonlinear multiple wave-number simulation”. *Nucl. Fusion* 62.1 (2022), p. 016012.
- [29] FREDRICKSON, E.D. “Excitation of toroidally localized harmonics of global Alfvén eigenmodes”. *Nucl. Fusion* 63.7 (2023), p. 076006.
- [30] BELOVA, E.V. “Full nonlinear simulations of GAEs in NSTX-U”. IAEA Fusion Energy Conference (London, UK, 2023). P/7 2393.
- [31] SABBAGH, S.A. et al. “Disruption event characterization and forecasting in tokamaks”. *Phys. Plasmas* 30.3 (2023), p. 032506.
- [32] ZAMKOVSKA, V. “DECAF cross-device exploration of disruption characterization indicated by abnormalities in plasma current and vertical position”. IAEA Fusion Energy Conference (London, UK, 2023). P/3 1909.
- [33] PICCIONE, A. et al. “Predicting resistive wall mode stability in NSTX through balanced random forests and counterfactual explanations”. *Nucl. Fusion* 62.3 (2022), p. 036002.
- [34] BERKERY, J.W. et al. “Density limits as disruption forecasters for spherical tokamaks”. *Plasma Phys. Control. Fusion* 65.9 (2023), p. 095003.
- [35] de VRIES, P.C. et al. “Cross-machine comparison of runaway electron generation during tokamak start-up for extrapolation to ITER”. *Nucl. Fusion* 63.8 (2023), p. 086016.
- [36] WAI, J.T., BOYER, M.D., and KOLEMEN, E. “Neural net modeling of equilibria in NSTX-U”. *Nucl. Fusion* 62.8 (2022), p. 086042.
- [37] AL KHAWALDEH, H. et al. “Model-based linear–quadratic–integral controller for simultaneous regulation of the current profile and normalized beta in NSTX-U”. *Fusion Eng. Des.* 192 (2023), p. 113795.
- [38] LEARD, B.R. et al. “Fast model-based scenario optimization in NSTX-U enabled by analytic gradient computation”. *Fusion Eng. Des.* 192 (2023), p. 113606.
- [39] EMDEE, E.D. and GOLDSTON, R.J. “The effect of gas injection location on a lithium vapor box divertor in NSTX-U”. *Nucl. Fusion* 63.9 (2023), p. 096003.
- [40] SOUKHANOVSKII, V.A. “Modeling of radiation transport effects in lithium divertors”. IAEA Fusion Energy Conference (London, UK, 2023). P/6 1913.
- [41] KHODAK, A. and MAINGI, R. “Plasma facing components with capillary porous system and liquid metal coolant flow”. *Phys. Plasmas* 29.7 (2022), p. 072505.
- [42] MAINGI, R. “Progress in a US-based liquid metal plasma-facing component design activity for a fusion nuclear science facility”. *IAEA Fusion Energy Conference*. TEC/2 2334. 2023.
- [43] LOOBY, T. et al. “3D ion gyro-orbit heat load predictions for NSTX-U”. *Nucl. Fusion* 62.10 (2022), p. 106020.
- [44] ZHANG, X. et al. “Reduced physics model of the tokamak Scrape-Off-Layer for pulse design”. *Nucl. Mater. Energy* 34 (2023), p. 101354.
- [45] GAN, K.F. et al. “Impact of edge harmonic oscillations on the divertor heat flux in NSTX”. *Phys. Plasmas* 29.1 (2022), p. 012503.
- [46] GAN, K.F. “The effect of intermittent divertor filaments on the divertor heat flux in NSTX”. IAEA Fusion Energy Conference (London, UK, 2023). P/9 2278.
- [47] LAMPERT, M. et al. “Internal rotation of ELM filaments on NSTX”. *Phys. Plasmas* 29.10 (2022).
- [48] LAMPERT, M., DIALLO, A., and ZWEBEN, S.J. “Novel angular velocity estimation technique for plasma filaments”. *Rev. Sci. Instrum.* 94.1 (2023), p. 013505.
- [49] ZWEBEN, S.J. et al. “Correlation between the relative blob fraction and plasma parameters in NSTX”. *Phys. Plasmas* 29.1 (2022), p. 012505.
- [50] ZWEBEN, S.J., LAMPERT, M., and MYRA, J.R. “Temporal structure of blobs in NSTX”. *Phys. Plasmas* 29.7 (2022), p. 072504.
- [51] BISAI, N. et al. “Experimental validation of universal plasma blob formation mechanism”. *Nucl. Fusion* 62.2 (2022), p. 026027.